Phonon polaritons in thin films and microcrystals of MnO

1989 J. Phys.: Condens. Matter 1 10351

(http://iopscience.iop.org/0953-8984/1/51/009)

J. Phys.: Condens. Matter **1** (1989) 10351–10359. Printed in the UK

Phonon polaritons in thin films and microcrystals of MnO

Shōsuke Mochizuki
Department of Physics, College of Humanities and Sciences, Nihon University, 3-25-40 Sakurajosui, Setagaya-ku, Tokyo 156, Japan

Received 13 February 1989, in final form 22 May 1989

Abstract. The infrared spectra of the MnO bulk, thin-film and microcrystal specimens are measured at room temperature by reflection and transmission methods. The reststrahlen reflectivity spectrum of MnO bulk crystal is analysed by means of a two-damped-oscillator dispersion model and the lattice vibrational properties of MnO are discussed. The virtual mode spectra of MnO thin film are analysed by means of the virtual mode theory of the anharmonic ionic crystal slab and the upper branch of the polariton dispersion curve of MnO at room temperature is determined experimentally for the first time. The extinction spectrum of MnO microcrystals is discussed in the light of the theory for the surface phonon polaritons in ionic microcrystals. The effects of the microcrystal–substrate interaction and the aggregation of microcrystals are also discussed.

1. Introduction

In recent years, considerable attention has been given to both the theoretical and the experimental investigation of the physical properties of finite-size crystals, thin films and microcrystals. Although the optical method is frequently used in experimental studies, the details of the photo-response of finite-size crystals are not fully elucidated. It is thus desirable to measure the optical spectra of both thin-film and microcrystal specimens, together with a bulk specimen of the same material which is used as a reference specimen. The infrared optical properties of the 3d transition-metal monoxides MnO, FeO, CoO and NiO and of the 4f rare-earth metal oxide CeO_2 have been measured in order to study the lattice vibrations and the photon–phonon interactions (Mochizuki and Satoh 1981, Mochizuki 1982, 1984, 1985, 1987, 1988) by using the bulk, thin-film and microcrystal specimens. The present paper is the result of work which had as its main purpose the experimental clarification of the phonon polariton modes in MnO.

MnO has the NaCl structure above the Néel temperature (118 K) but, below the Néel temperature, the crystal transforms to an antiferromagnetic structure which is slightly distorted from the ideal NaCl structure. Since the distortion is quite small, it is frequently supposed that the phonon spectrum does not depend on the magnetic ordering. The infrared optical properties of MnO are governed by the vibrational modes in which the sublattice of the Mn ions moves opposite to that of the O ions. Such a motion is associated with strong electric moments and hence interacts directly with the electric field of the incident radiation. This interaction leads to the formation of polariton modes.

0953-8984/89/5110351 + 09 $02.50

The polariton modes decay after a certain time through photon (at the surface) and phonon (in the bulk) emission processes. The polaritons in bulk crystals propagate as plane waves because of the translational symmetry of the lattice.

Only a few studies concerning the reststrahlen spectrum of MnO (Plendl *et al* 1969, Kinney and O'Keeffe 1969) have been reported. They show, however, some differences in the dielectric and dispersion parameters. In thin-film crystals, the polariton modes are somewhat complicated. The optical properties of an ionic crystal thin film were first studied by Berreman (1963) for LiF and were discussed by Fuchs and Kliewer (1965, 1966) from the viewpoint of Maxwell's equations. The theory is valid when the thickness of the thin film is much smaller than the wavelength of the incident infrared radiation and larger than the inter-atomic spacing. The finite thickness of the film causes two types of modes:

(i) non-radiative modes with exponentially damped fields outside the film;
(ii) radiative modes with incoming or outgoing oscillatory polarised waves outside the film.

The radiative modes are accessible to the usual optical measurements and it is argued that they are virtual modes. The observation of the radiation due to the virtual modes is made in the region of $\omega > ck$ in the ω–k_x plane, where ω is the virtual mode frequency, c is the speed of light in free space and k_x the x component of the wavevector k; the x axis is parallel to the specimen layer. The virtual mode equations for p-polarised radiation from a parallel-flat specimen of thickness $d = 2a$, at an oblique angle θ, are

$$-\mathrm{i}\varepsilon\beta_0/\beta = \tan(\beta a) \tag{1}$$

$$\mathrm{i}\varepsilon\beta_0/\beta = \cot(\beta a) \tag{2}$$

$$\beta_0 = \sqrt{(\omega/c)^2 - k_x^2} \tag{3a}$$

$$\beta = \sqrt{(\omega/c)^2\varepsilon - k_x^2} \tag{3b}$$

$$k_x = (\omega \sin\theta)/c \tag{3c}$$

where ε is the frequency-dependent dielectric constant of the thin-film material. For $\varepsilon\beta_0/\beta > 1$, the tangent equation (1) has solutions corresponding to $\beta\mathrm{d} \simeq (n + \frac{1}{2})\pi$, where n is an integer, and the cotangent equation (2) has solutions for $\beta\mathrm{d} \simeq n\pi$. These solutions are labelled as nTH, nTL, nCH and nCL: n is the above-mentioned integer, T or C indicates that the characteristic equation is tangent type or cotangent type, and H or L indicates the high-frequency or low-frequency solution. For very thin films, $d \ll c/\omega_T$, these virtual mode equations give the following solutions:

(i) 0TH mode centred near the longitudinal optical (LO) phonon frequency ω_L;
(ii) 2TL mode centred near the transverse optical (TO) phonon frequency ω_T of the film material.

The 0TH mode and 2TL mode correspond to the polarisation perpendicular and parallel, respectively, to the specimen layer. Since k_x varies with the incident angle, these virtual mode frequencies are dependent on θ, therefore the upper branch of the polariton dispersion curve is experimentally determined by measuring the dependence on the angle of incidence of the reflection spectrum due to the 0TH mode. In the present study, we measured the virtual mode spectra at various angles of incidence and determined the upper branch of the polariton dispersion curve for MnO. In micro-crystals, the polaritons can no longer propagate in the form of a plane wave because of

lack of translational symmetry at the surface. Treating the microcrystals as a dielectric continuum which is characterised by a local frequency-dependent dielectric constant, we find that a subset of solutions of Maxwell's equations is classified as the surface polaritons. For example, Englman and Ruppin (1968) have shown that, in a spherical crystal of small radius R, surface modes exist. In the limiting case $\omega R/c < 1$, the frequencies of these modes are determined from the equation

$$\varepsilon(\omega) = -(l+1)\varepsilon_m/l \qquad l = 1, 2, 3, \ldots \tag{4}$$

where $\varepsilon(\omega)$ is the dielectric constant of the microcrystal material and ε_m the dielectric constant of the medium surrounding the microcrystal. The surface modes cause optical absorption in the frequency region from the TO phonon frequency to the LO phonon frequency. However, in real optical experiments on microcrystals the situation is complicated by the large number of interacting microcrystals (Clippe and Lucas 1976), by the presence of distributions of microcrystal shape and microcrystal size, and by the presence of a substrate (Ruppin 1983). In the present study, we measure the surface polariton mode spectra of MnO microcrystals and examine these effects.

So far as we know, this is a first report of the infrared optical properties of thin films and microcrystals of MnO.

2. Experimental details

Nominally pure single-crystal boules of MnO were grown by the Verneuil method. Many MnO plates were obtained by slicing the boules along the cleavage plane and were examined by x-ray analysis, infrared spectroscopy and microscopy observation. We selected the crystals which do not show the presence of some higher-oxidation states of Mn. The crystals were annealed for 3 h at 1273 K in a 10% H_2–90% Ar atmosphere, which yields fully reduced MnO. In the past, such care has been seldom used in the infrared studies of MnO.

The metal-backed MnO thin-film specimens were produced as follows. The manganese films were made by evaporating the manganese of 99.99% purity from a heated alumina crucible onto a smooth surface of platinum substrate whose reflectivity is close to that of evaporated gold plane mirror in the frequency range from 250 to 1000 cm^{-1}. The evaporated manganese on platinum substrates were then oxidised for several hours at 673 K in an O_2 atmosphere and were reduced for several hours at 673 K in a 10% H_2–90% Ar atmosphere, which yields light-green thin-film MnO backed by platinum. Examination using an x-ray diffractometer indicated the thin films thus obtained to be polycrystalline MnO. Although a variety of methods—the halide decomposition method (Cech and Alessandrini 1959), the vapour deposition method (Huffman *et al* 1969) and sputtering of MnO—have been used to try to form MnO films in our laboratory, large-area metal-backed MnO layers with various thicknesses are produced more easily by this controlled oxidation–reduction method. The microcrystals were produced by pulverising the MnO single crystal or by reducing MnO_2 microcrystals for several hours at 1273 K in a 10% H_2–90% Ar atmosphere. The crystallites were found to be polyhedra of sizes ranging from 10 to 100 nm. They were dispersed in polyethylene by the usual infrared sample preparation technique; the filling factor was 0.001. To study the effects of the microcrystal–substrate interaction and the aggregation of microcrystals, the microcrystals were dispersed in helium gas and collected on a KRS-5 plate or a gold-evaporated plane mirror.

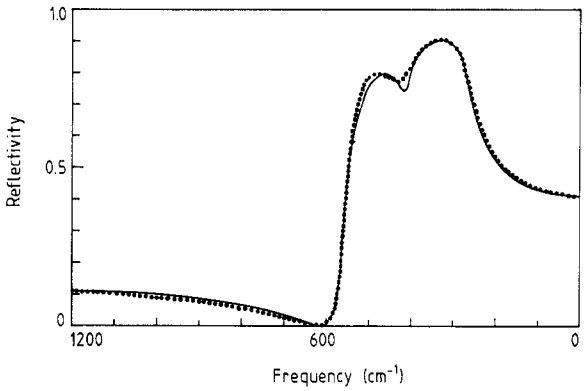

Figure 1. Reflectivity of MnO at room temperature: ●, observed values; ——, reflectivity spectrum calculated using the two-damped-oscillator model.

We made infrared measurements using a double-beam grating spectrophotometer (Hitachi-295). Several optical systems in the specimen chamber were chosen. A quasi-normal angle-of-incidence reflection optical system and a variable angle-of-incidence reflection optical system were designed and constructed in our laboratory. A grid-type polariser (Cambridge Physical Science IGP-225) was used for the polarisation measurements. No corrections were made for incomplete polarisation of the beam caused either by polariser imperfection or by incomplete collimation of the beam (angular aperture, less than 10°).

The far-infrared measurements in the frequency range from 2 to 250 cm^{-1} at the synchrotron orbital radiation beam line BL6A1 of the Institute for Molecular Science and by using grating spectrophotometers.

3. Results and discussion

We measured the reflectivity spectra of MnO single crystals at room temperature before and after the heat treatment at 1273 K in a 10% H_2–90% Ar atmosphere in the frequency range from 7 to 4000 cm^{-1}. Typical results for the frequency range from 7 to 1200 cm^{-1} are shown by the full circles in figure 1. The shape of the reflectivity spectrum in the spectral region from 350 to 550 cm^{-1} is specimen dependent. Independent determination of the far-infrared reflectivity spectrum was made by calculating the reflectivity for normal incidence using the optical constants obtained from the spectra caused by multiple reflection in a thin MnO single crystal. We performed an oscillator fit with the complex dielectric constant $\varepsilon(\omega) = \varepsilon_1(\omega) - i\varepsilon_2(\omega)$ given by

$$\varepsilon(\omega) = [n(\omega) - ik(\omega)]^2 = \varepsilon(\infty) + \sum_j \frac{S_j\omega_j^2}{\omega_j^2 - \omega^2 + i\omega\Gamma_j} \tag{5}$$

where $n(\omega)$ and $k(\omega)$ are the real and imaginary parts of the complex refractive index $N(\omega)$, $\varepsilon(\infty)$ is the high-frequency dielectric constant, ω_j is the resonance frequency, Γ_j is the damping constant and S_j is the oscillator strength of the infrared-active jth oscillator. The static dielectric constant $\varepsilon(0)$ is then

$$\varepsilon(0) = \varepsilon(\infty) + \sum_j S_j. \tag{6}$$

Table 1. Dispersion parameters of MnO.

	ω_1 (cm^{-1})	ω_2 (cm^{-1})	S_1	S_2	Γ_1/ω_1	Γ_2/ω_2	$\varepsilon(0)$	$\varepsilon(\infty)$
This work	270.3	417.0	15.70	0.2368	0.0950	0.1274	20.89	4.95
Plendl *et al* (1969)	262	445	17.5	0.05	0.092	0.088	22.50	4.95

The reflectivity $R(\omega)$ for normal incidence is given by

$$R(\omega) = \{[n(\omega) - 1]^2 + k(\omega)^2\}/\{[n(\omega) + 1]^2 + k(\omega)^2\}. \tag{7}$$

Using the above equations, we determine the values of the dispersion parameters ω_j, Γ_j and S_j so as to obtain the best overall fit between the observed and calculated reststrahlen curves. A good fit as indicated by the full curve in figure 1 was obtained using two damped oscillators with parameters which are compared in table 1 with those of Plendl *et al* (1969) (and also with those of Kinney and O'Keeffe (1969)). Agreement between both sets of parameters is satisfactory.

A MnO crystal at room temperature has the NaCl structure with three optical branches. The transverse optical phonon branch at zero wavevector, $q = 0$, gives rise to intense infrared absorption. The main ω_1 resonance at 270.3 cm^{-1} is thus identified with the TO phonon mode near the centre of the Brillouin zone. The LO phonon frequency ω_L at $q = 0$ obtained from the Lyddane–Sachs–Teller relation is 555.2 cm^{-1}. It is close to the value of 563.6 cm^{-1} defined as the frequency where ε_1 vanishes. The subsidiary resonance at 417.0 cm^{-1} may be attributed to the process involving phonon–phonon interactions due to the second-order dipole moment and the anharmonic potential. The total effective ionic charge calculated from the Szigeti (1949) relation is 1.10, which is larger than the value for CoO or NiO (Gielisse *et al* 1965); MnO may suffer a smaller deformation of the electron clouds because of the short-range force of the neighbouring ions than those in CoO and NiO.

The reflection spectra of MnO thin-film specimens of various thicknesses on the smooth-surface platinum substrate were measured at various angles of incidence from 12.5 to 87.5° at room temperature. The reflection spectra of the metal-backed MnO thin film of 600 nm thickness at an angle of incidence of 30° are shown in figure 2(*a*). We determined the reflectivity by comparison with the reflectivity of a platinum substrate without a MnO film. As seen in figure 2(*a*), the p-polarised spectrum consists of two reflection minimum bands centred at about 555 and 250 cm^{-1}, while the s-polarised spectrum has only a reflection minimum band centred at about 250 cm^{-1}. The virtual mode theory (Fuchs and Kliewer 1965, 1966) tells us that the band centred at about 555 cm^{-1}, which is close to the LO phonon frequency of the MnO bulk crystal, is due to the 0TH virtual mode and that the band centred at about 250 cm^{-1}, which is near to the TO phonon frequency of the MnO bulk crystal, is due to the 2TL virtual mode. It was frequently noted that, for the MnO thin-film specimen containing some Mn_3O_4, the band due to the 0TH mode is accompanied by a sub-band centred at about 595 cm^{-1}. The shape and the central frequency of this sub-band are not changed by the angle of incidence nor by the polarisation of the incident radiation.

The reflectivity spectrum R can be theoretically calculated from the theory of Fuchs and Kliewer (1965, 1966). We calculated the reflectivity spectra of the metal-backed MnO thin film of 600 nm thickness using the dielectric constant $\varepsilon(\omega)$ obtained in the present study. The result is shown in figure 2(*b*). The calculation reproduces the overall

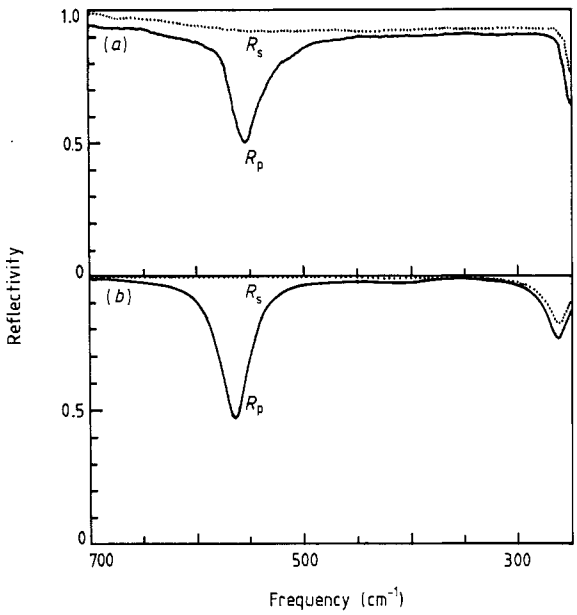

Figure 2. (*a*) Experimental and (*b*) theoretical reflectivity spectra of a MnO thin film 600 nm thick on a platinum substrate at room temperature at 30° incidence: ——, spectra for p-polarised radiation; ·····, spectra for s-polarised radiation.

behaviour rather well but fails badly in predicting the magnitude and central frequencies of the absorption due to the virtual modes. This may arise from the dielectric function determined by analysing the reflectivity data or from the difference between the lattice vibrational properties of the thin-film specimen and those of the bulk specimen.

Using the same specimen, we studied the dependence of the angle of incidence of the 0TH mode at room temperature. Three spectra are shown in figure 3. It is seen in this figure that, as the angle of incidence increases, the central frequency of the 0TH mode shifts to a higher frequency and the width of the band increases. The central frequency of the 0TH mode is theoretically given as one of the solutions in the tangent-type equation (1). Using equations (1) and (3), we can determine experimentally the upper branch of the polariton dispersion curve. Figure 4 shows the upper branch of the polariton dispersion curve of MnO at room temperature. The open circles and the full curve represent the experimental and theoretical curves, respectively. The theoretical curve was calculated with the following dispersion parameters:

$$\varepsilon(0) = 20.89 \qquad \varepsilon(\infty) = 4.95 \qquad \omega_T = 270.3\ \text{cm}^{-1}.$$

As shown in this figure, the experimental results agree fairly well with the theoretical dispersion curve, although we ignored the effect of the phonon damping due to the lattice anharmonicity.

Finally we show the phonon polariton modes of MnO microcrystals. The transmissivity spectrum of MnO microcrystals embedded in polyethylene were measured at room temperature in the frequency range from 250 to 700 cm^{-1}. By considering the specimen as a composite optical medium, we write the transmissivity $T(\omega)$

$$T(\omega) = [1 - R(\omega)]^2 \exp[-K(\omega)d] \tag{8}$$

where $R(\omega)$ is the reflectivity, $K(\omega)$ is the extinction and d is the thickness of the composite optical medium. Also, since as a dielectric medium polyethylene has some absorption bands $K_p(\omega)$, it may be appropriate to assume the extinction $K_m(\omega)$ for the

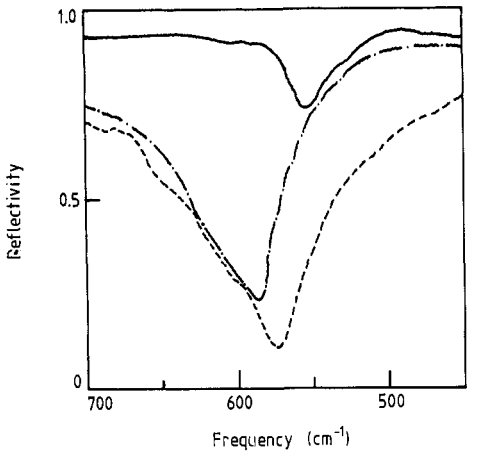

Figure 3. Reflectivity spectra due to the 0TH mode in a MnO thin film on a platinum substrate at room temperature for several angles of incidence: ——, $\theta = 20.0°$; —·—, $\theta = 87.5°$; ----, $\theta = 80.0°$.

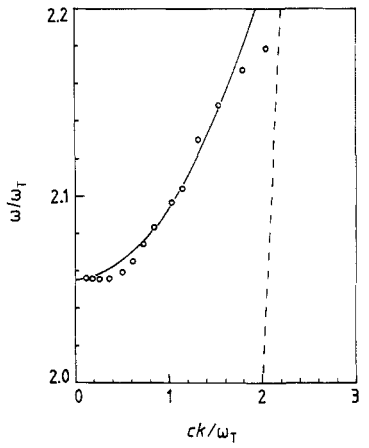

Figure 4. Upper branch of the polariton dispersion curve of MnO at room temperature: ○, experimental data; ——, calculated curve.

microcrystals embedded in non-absorbing medium to be of the following form:

$$K_m(\omega) = K(\omega) - K_p(\omega). \tag{9}$$

Using these relations, we determined the extinction spectrum of MnO microcrystals at room temperature from the transmissivity data. The result is shown in figure 5. The extinction spectrum shows a broad band between the TO phonon and LO phonon frequencies of the MnO bulk crystal. The broad band centred at 350 cm^{-1} shifts to lower frequencies with increasing dielectric constant of the surrounding medium. Thus we can assign the broad band to the surface phonon polariton mode in MnO microcrystals. The peak frequency of 350 cm^{-1} is a fair way below the limiting frequency of 450 cm^{-1} of an ideal spherical MnO microcrystal; the frequency was determined from equation (4) for $l = 1$. The observed band is much broader than that calculated using a continuum model (Genzel and Martin 1972) with the dielectric constant of the MnO bulk crystal obtained in the present study. For the broad band width of ionic microcrystals, various tentative explanations have been given on the basis of the continuum model by taking the size distribution, the particle aggregation, the enhanced phonon scattering and the non-spherical shape. With respect to the optical absorption of cubic MgO microcrystals,

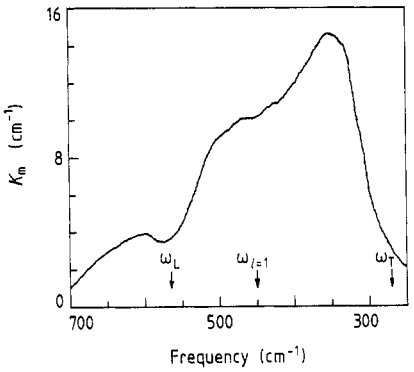

Figure 5. Extinction spectrum of MnO microcrystals at room temperature. The frequencies ω_L, ω_T and $\omega_{l=1}$ with arrows indicate the LO phonon frequency, the TO phonon frequency and the frequency determined by equation (4) for $l = 1$, respectively.

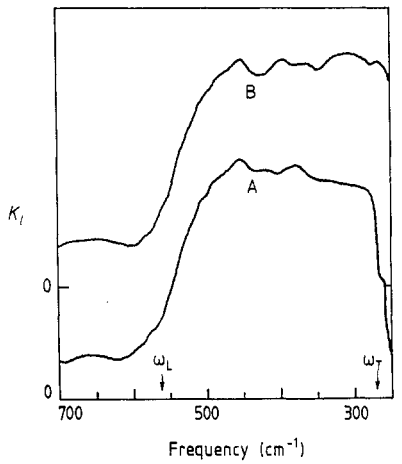

Figure 6. Extinction spectra of MnO microcrystals on a KRS-5 substrate (curve A) and on a gold-evaporated plane mirror substrate (curve B).

Fuchs (1975, 1978) has quantitatively explained fairly well the experimental broad spectrum by taking into account the crystal shape, without unphysically high phonon damping, and Matumura and Cho (1981) have also explained their broad spectra by assuming spherical coagulation of the microcrystal with the same dielectric constant as that of a bulk crystal. According to microscopic observation of our microcrystal specimen, the crystallites are found to be polyhedra and it is frequently seen that the polyhedral microcrystals embedded in polyethylene aggregate into clusters with dimensions ranging from several tenths of micrometres to several micrometres. Although it is difficult to calculate exactly the extinction spectrum of polyhedral microcrystals, the above result for cubic MgO suggests that the non-spherical (polyhedral) shape leads to splitting of the surface phonon polariton modes. Therefore, such splitting of the surface phonon polariton modes and coagulation of the microcrystals may cause the broad extinction band shown in figure 5. In optical experiments on microcrystals, the situation is often complicated by the presence of the substrate on which they are deposited. To study this, we measured the room-temperature transmissivity $T(\omega)$ and reflectivity $R(\omega)$ spectra of the same MnO microcrystals deposited on a KRS-5 and a gold-evaporated plane mirror, respectively, as quasi-normal-incidence. By considering the microcrystal layer as a composite optical medium, we determined the extinction spectra for these specimens from the following equations (Mochizuki 1982):

$$T(\omega) = [1 - R_l(\omega)]^2 \exp[-K_l(\omega)d] \tag{10}$$

$$R(\omega) = [1 - R_l(\omega)]^2 \exp[-2K_l(\omega)d] \tag{11}$$

where $R_l(\omega)$, $K_l(\omega)$ and d are the reflectivity, the extinction and the thickness, respectively, of the microcrystal layer. The result is shown in figure 6. As seen in this figure, the spectra consist of a weak narrow band centred at the TO phonon frequency of the MnO bulk crystal and a broad band in the frequency region between the TO phonon and LO phonon frequencies of the MnO bulk crystal. Since the weak band at the TO phonon

frequency disappears in the spectrum of the microcrystal specimen dispersed in polyethylene, we attribute it to a cylindrical cluster mode of the MnO microcrystals. The broad extinction band shifts to lower frequencies when the KRS-5 substrate is replaced with a gold-evaporated substrate. This feature agrees qualitatively with the theoretical study of surface modes and optical absorption of a spherical microcrystal on a substrate (Ruppin 1983). On the basis of this theory, the broad structureless extinction may be attributed to the distributions of the microcrystal size and of the separation of the microcrystal and substrate.

Acknowledgments

This work was partially supported by the Fund for Science Promotion of Nihon University. This work was also supported by the Joint Studies Program (1987–9) of the Institute for Molecular Sciences. I wish to thank Professor R Ruppin for helpful discussions.

References

Berreman D W 1963 *Phys. Rev.* **130** 2193
Cech R E and Alessandrini E I 1959 *Trans. Am. Soc. Met.* **51** 150
Clippe P and Lucas A 1976 *Phys. Rev.* B **14** 1715
Englman R and Ruppin R 1968 *J. Phys. C: Solid State Phys.* **1** 614, 630, 1515
Fuchs R 1975 *Phys. Rev.* B **11** 1732
—— 1978 *Phys. Rev.* B **18** 7160
Fuchs R and Kliewer K L 1965 *Phys. Rev.* **140** A2076
—— 1966 *Phys. Rev.* **144** 495; **150** 573; **150** 589
Genzel L and Martin T P 1972 *Phys. Status Solidi* b **51** 91
Gielisse P J, Plendl J N, Mansur L C, Marshall R, Mitra S S, Mykolajewycz R and Smakula A 1965 *J. Appl. Phys.* **36** 2446
Huffman D R, Wild R L and Shinmei M 1969 *J. Chem. Phys.* **50** 4092
Kinney T B and O'Keeffe M O 1969 *Solid State Commun.* **7** 977
Matumura O and Cho M 1981 *J. Opt. Soc. Am.* **71** 393
Mochizuki S and Satoh M 1981 *Phys. Status Solidi* b **106** 667
Mochizuki S 1982 *Phys. Status Solidi* b **110** 219
—— 1984 *Phys. Status Solidi* b **126** 105
—— 1985 *Phys. Status Solidi* b **128** 23
—— 1987 *Proc. Inst. Nat. Sci. Nihon Univ.* **22** 63
—— 1988 *Phys. Status Solidi* b **145** K75
Plendl J N, Mansur L C, Mitra S S and Chang L F 1969 *Solid State Commun.* **7** 109
Ruppin R 1983 *Surf. Sci.* **127** 108
Szigeti B 1949 *Trans. Faraday Soc.* **45** 155